Paper No. 901. (quote when citing this article)
Eleventh World Conference on Earthquake Engineering
ISBN: 0 08 042822 3

WIDE BAND STRONG MOTION RECORDS DURING THE 1994 HOKKAIDO TOHO-OKI EARTHQUAKE (M8.1)

T. SASATANI, M. FURUMURA, S. SAITO and H. NAGUMO

Division of Earth and Planetary Sciences, Graduate School of Science,
Hokkaido University, Sapporo 060, Japan

ABSTRACT

We analyze wide band strong motion records during the 1994 Hokkaido Toho-Oki earthquake (M_{JMA} 8.1) and its largest aftershock (M_{JMA} 7.3), observed at 4 sites (Δ=270~380 km) in the south-eastern part of Hokkaido, Japan. By comparing the wide band records from the main shock with those from the largest aftershock over the wide period range (0.05 ~ 100 s), we extract unique source process of the 1994 Hokkaido Toho-Oki earthquake. The unique points derived from our analyses are: 1) large centroid depth, 2) high moment release density, 3) existence of ripples with a period of several seconds in the P-wave portion on the vertical velocity records, 4) anomalously strong radiation of short-period (less than 0.5 s) seismic waves. These indicate that the 1994 Hokkaido Toho-Oki earthquake rupture a substantial part of the subducting oceanic lithosphere radiating anomalously strong short-period seismic waves.

KEYWORDS

The 1994 Hokkaido Toho-Oki earthquake; Wide band strong motion records; Ripples in seismograms; Moment release density; Lithospheric earthquake.

INTRODUCTION

A large earthquake (M_{JMA} 8.1) occurred far east off Hokkaido on October 4, 1994 (Fig. 1). This earthquake is named as the 1994 Hokkaido Toho-Oki earthquake by JMA (Japan Meteorological Agency). A large tsunami and strong shaking caused severe damage to the eastern part of Hokkaido and the southern part of the Kurile islands. This earthquake is characterized by an extremely large felt area, and by observed peak horizontal accelerations being much larger than those expected from the empirical attenuation relation. We take an interest in these characteristics and study wide band strong motion records during this large earthquake to understand reasons for them.

Kikuchi and Kanamori (1995) have studied the source process of the 1994 Hokkaido Toho-Oki earthquake using far-field body-waves (P and SH components) and long-period Love and Rayleigh waves. Their results are summarized as follows: 1) the mechanism is clearly different from those of the large earthquakes in this region that had occurred on the subduction plate boundary (Fig. 1), 2) the large centroid depth (56 km) and the high stress drop (11MPa) strongly suggest that the 1994 Hokkaido Toho-Oki earthquake is a lithospheric

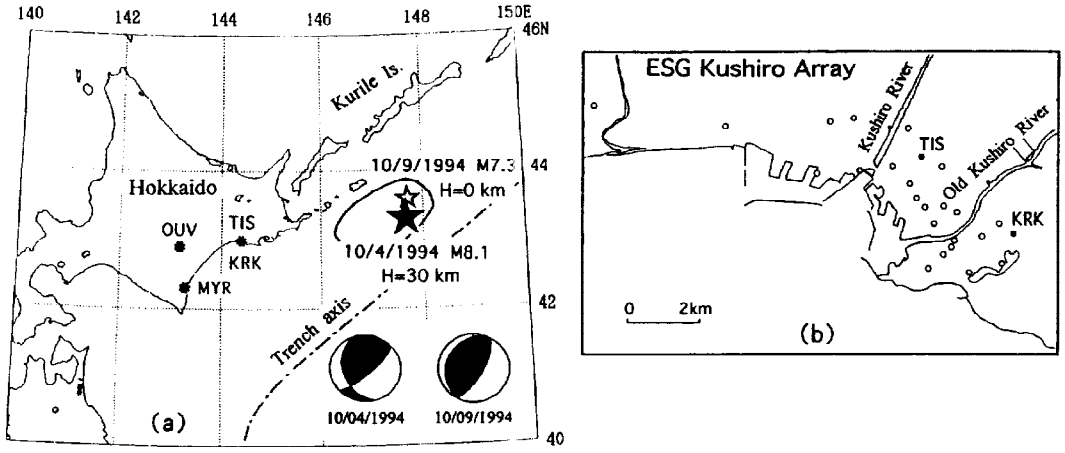

Fig. 1. (a) Location map showing epicenters of the 1994 Hokkaido Toho-Oki earthquake (★) and its largest aftershock (☆), and observation sites (●). The focal parameters are taken from JMA. Also shown are their focal mechanisms. (b) ESG cooperative strong motion observation sites in Kushiro city.

earthquake: an intra-plate event that rupture through a substantial part of the subducting oceanic lithoshpere. On the other hand, the largest aftershock (M_{JMA} 7.3) occurring on October 9, 1994 has the typical plate boundary mechanism in this region (Fig. 1).

Wide-band strong motions during this large event and many aftershocks were observed at 4 sites located in the south-eastern part of Hokkaido. Their epicentral distances are from 270 to 380 km. In this paper we analyze these records over the wide period range (0.05~100 s). By comparing the wide band strong motion records from the main shock with those from the largest aftershock, we will extract unique source process of the 1994 Hokkaido Toho-Oki earthquake. Hereafter we abbreviate the main shock and the largest aftershock to the 10/4 event and the 10/9 event, respectively.

DATA

Strong motion data used in this study were obtained at 4 observation sites in Hokkaido (Fig. 1). MYR is located on the rock site. OUV is located at the central part of the Tokachi plain which is the sedimentary basin covered mainly by terrace deposits. A thickness of the sedimentary layer beneath this site is about 600 m. TIS and KRK are located in Kushiro city and these belong to a part of the ESG Kushiro array (Sasatani, 1996). TIS is on the lowland with an alluvial thickness of about 100m, while KRK is on the hill zone. Wide frequency band, velocity-type strong motion seismometers (Muramatu, 1995) were installed at these stations: VS1(Tokyo Sokushin Co.) at TIS and VS3(Tokyo Sokushin Co.) at MYR,OUV and KRK. These have a wide flat response to ground velocity in the frequency range of 0.025 to 20 Hz (VS1) and 0.002 to 30 Hz (VS3).

Figures 2 and 3 show observed velocity seismograms during the 10/4 and 10/9 events. Unfortunately, the horizontal components are off-scaled at KRK during the 10/4 event. We use only the vertical component at this station in the following analysis. We can see different features among these seismograms depending on site conditions as mentioned above and event magnitudes. For example, the horizontal component seismograms at OUV have long duration later phases with a period of several seconds, which are interpreted as the basin transduced surface waves (Furumura and Sasatani, 1996). In the following sections, we analyze these records over the three period ranges: long-period seismic waves (10 - 100 s), intermediate-period seismic waves (1 - 10 s) and short-period seismic waves (0.05 - 1 s).

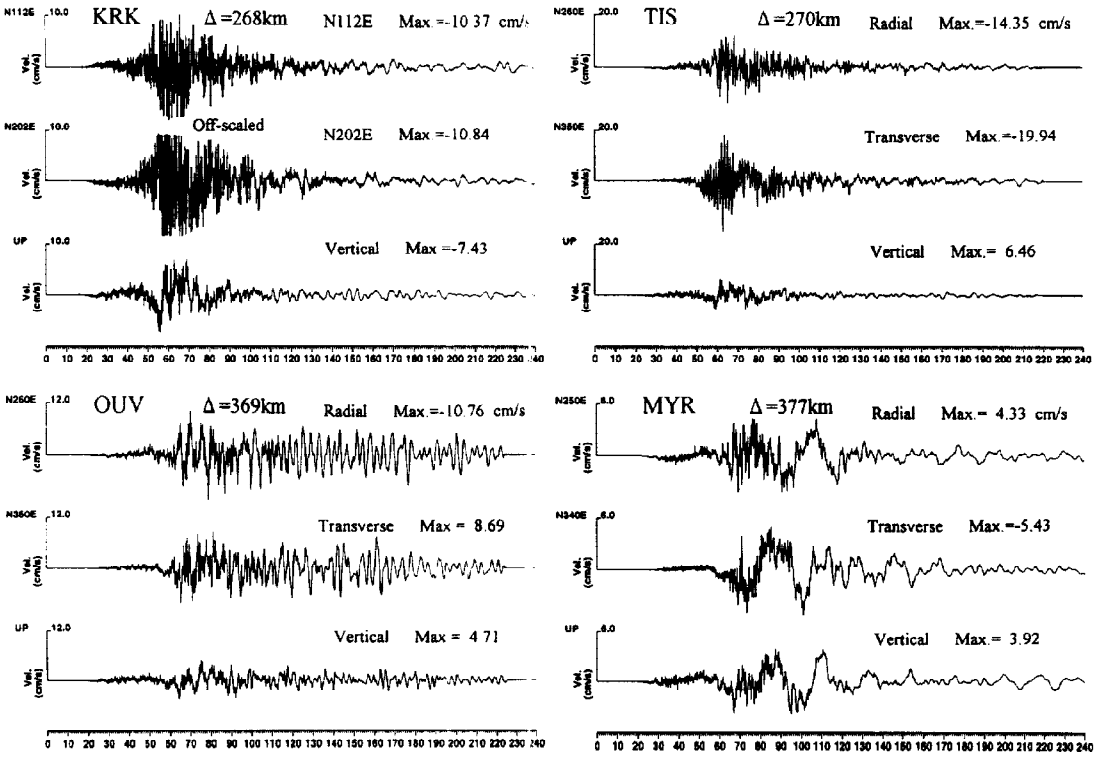

Fig. 2. Observed velocity seismograms at KRK, TIS, OUV and MYR during the Hokkaido Toho-Oki earthquake (10/4/1994).

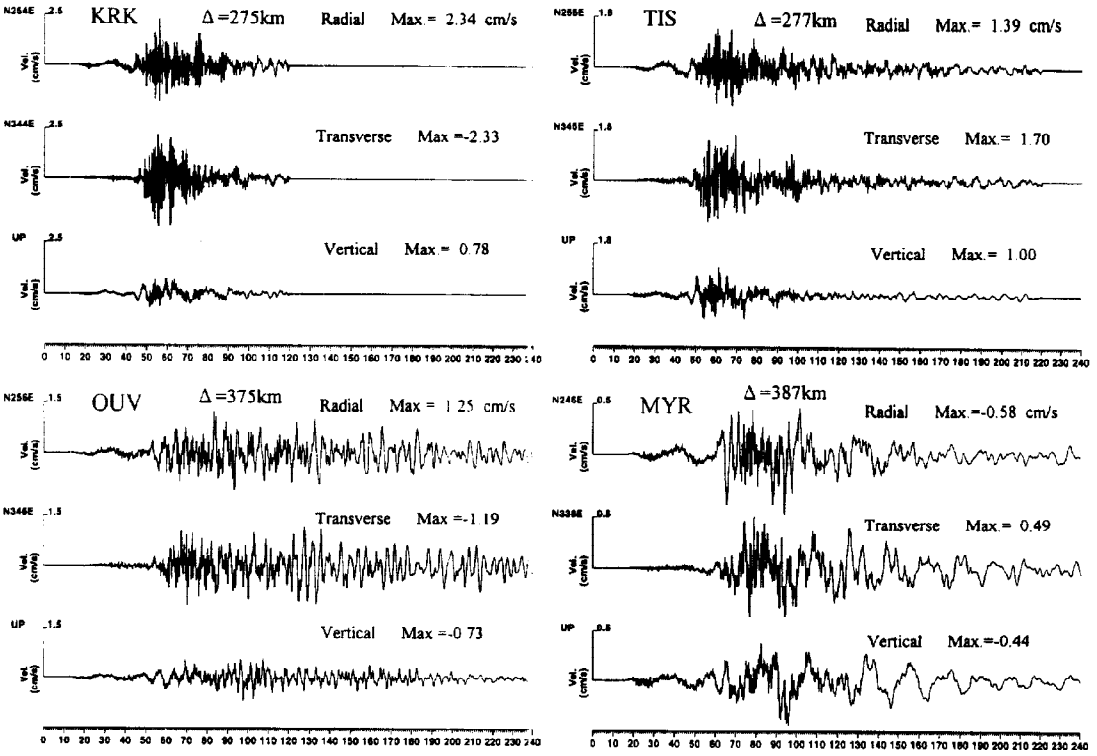

Fig. 3. Observed velocity seismograms at KRK, TIS, OUV and MYR during the largest aftershock(10/9/1994).

LONG-PERIOD SEISMIC WAVES

Here we analyze displacement seismograms obtained by integration of velocity records. Figure 4 shows displacement seismograms from the 10/4 and 10/9 events at the rock site MYR. S pulse shape on the transverse component is relatively simple and the pulse width for the 10/4 events is longer than that for the 10/9 event. Surface waves are predominant on the seismograms for the 10/9 event than those for the 10/4 event. These features provide information about the total source process. We calculate synthetic seismograms based on the mechanisms shown in Fig 1 and the flat layer crustal structure modified from the Kurile continental slope model by Iwasaki *et al.* (1989). In the calculation, we assume a point source with a parabolic ramp source time function. The synthetic seismograms calculated by changing the focal depth and the rise time of the parabolic ramp function (source process time) are compared with observed ones to estimate the reasonable source parameters. Figure 5 shows an example of comparison between observed and synthetic seismograms for the 10/4 event. An agreement is fairly good in spite of the simple calculation. Our final results are: (depth, H, source process time, T, seismic moment, Mo) = (50 km, 30 s, 3.7×10^{21}Nm) for the 10/4 event and (H, T, Mo) = (20 km, 15 s, 5.5×10^{19}Nm) for the 10/9 event. Important points are: 1) the 10/4 main shock with a distinct mechanism has the large centroid depth, while the 10/9 aftershock with a typical subduction mechanism has the considerably shallow depth; 2) moment release density (Mo/T) for the 10/4 event is extremely higher than that for the 10/9 event. Our results are nearly the same as those obtained by Kikuchi and Kanamori (1995).

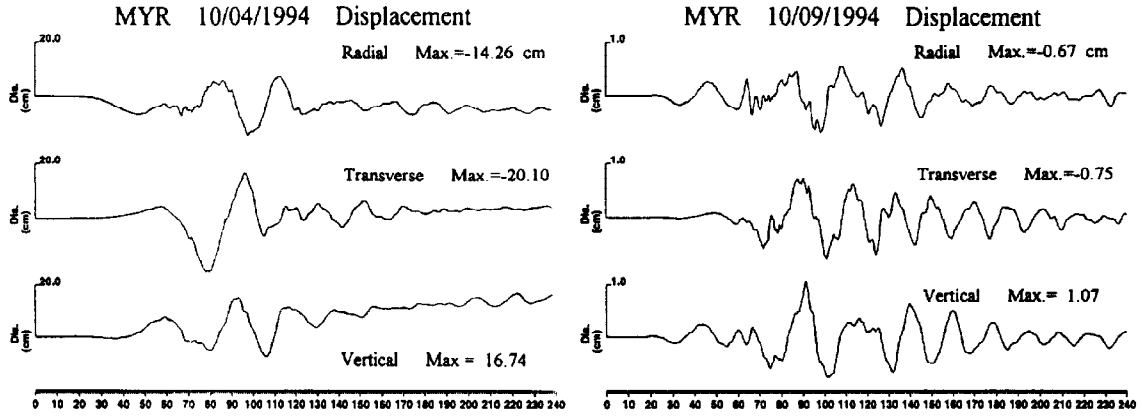

Fig. 4. Examples of displacement seismograms at MYR during the 10/4 event (left) and the 10/9 event (right).

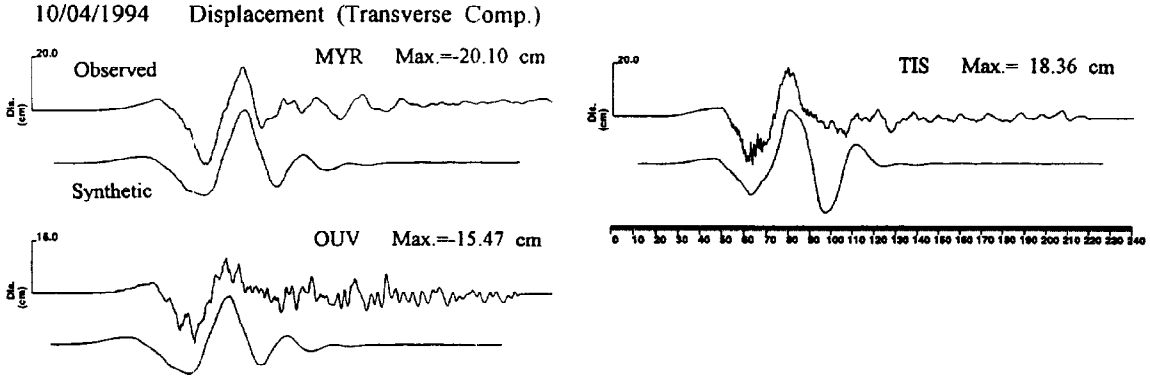

Fig. 5. Comparison between the observed and synthetic seismograms (transverse component) for the 10/4 event.

INTERMEDIATE-PERIOD SEISMIC WAVES

In order to extract more complex source process, we analyze velocity seismograms in which intermediate-period seismic waves predominate. Horizontal velocity seismograms are strongly affected by the site response and are not useful to directly extract source process information. On the other hand, the vertical components are not severely affected by the site response as demonstrated by Campillo *et al.* (1989). Here we analyze the vertical velocity seismograms to extract source process information. In the P-wave portion on the vertical velocity seismograms, interesting seismic waves with a period of several seconds are observed during the 10/4 event as shown in Fig. 6(a). We make high-cut filtered seismograms to clearly see these seismic waves (Fig. 7(b)). Since the 10/4 event has the source process time of about 30 s as obtained in the previous section, signals in the first 30 s duration may be direct P waves from the seismic source. At 4 sites they have a similar wave shape. Several ripples appear about 10 seconds after the initial small, smooth signal, superposed with a long-period undulation. Especially, the coherent ripples are observed at KRK, TIS and OUV: these stations have approximately the same direction from the epicenter. The original and the high-cut filtered vertical velocity seismograms for the 10/9 event are also shown in Figs. 6(b) and 7(b). On these seismograms, we do not see the clear, coherent ripples in the first 15 seconds duration. This fact indicates that the strong ripples observed during the 10/4 event is not due to a path effect, but due to a source effect.

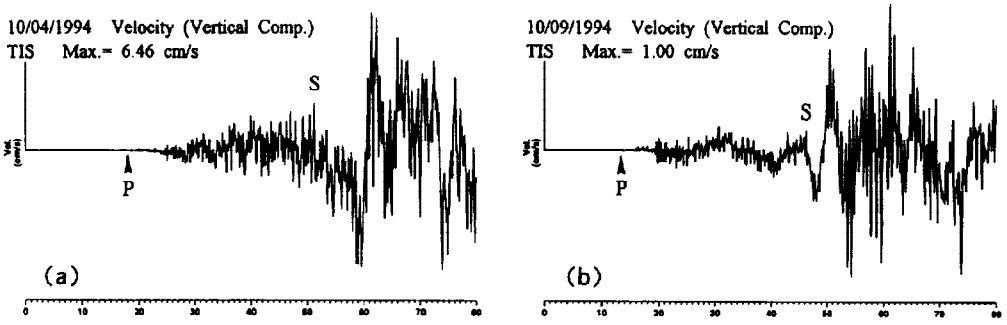

Fig. 6. An example of observed vertical velocity seismograms. (a) the 10/4 event and (b) the 10/9 event. P indicates the first P-wave arrival and S, approximate S-wave arrival.

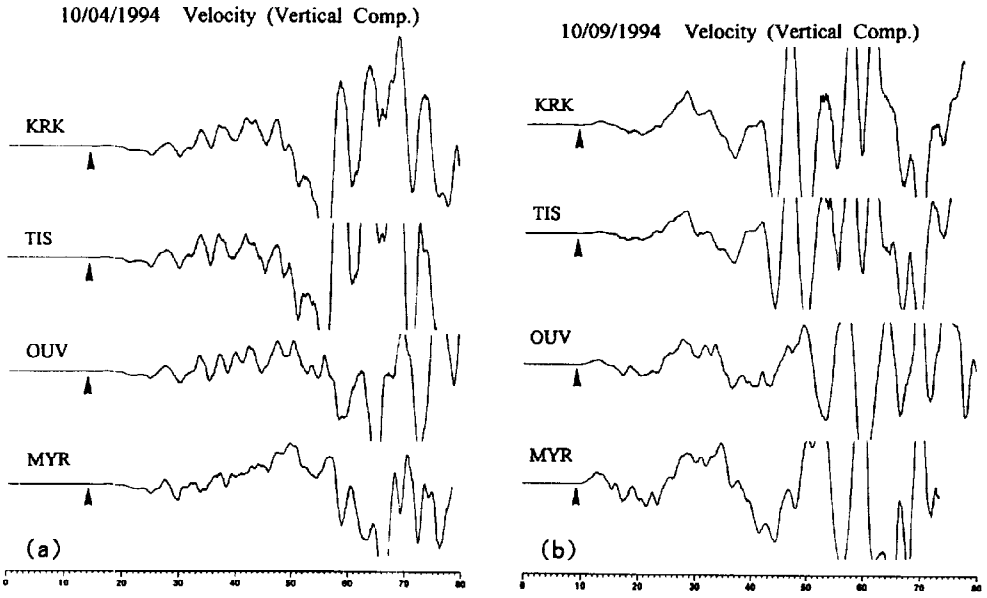

Fig. 7. High-cut filtered vertical velocity seismograms. (a) the 10/4 event and (b) the 10/9 event. Triangles indicate the first P-wave arrivals.

Kikuchi and Kanamori (1995) inverted 32 body wave records to determine the rupture pattern of the 10/4 event in terms of a series of subevents. They found 6 subevents during the 42 s source process time. Observed ripples on the vertical velocity seismograms for the 10/4 event may correspond to seismic signals from the series of subevents. Campillo *et al.*(1989) proposed a different model to explain the 3 s period ripples observed at Caleta de Campos during the 1985 Michoacan, Mexico earthquake: a self-similar crack model with a series of changes of the rupture front velocity. Since we have no near-field records, it is difficult to know which models is reasonable to explain the observed ripples. In any way, the existence of ripples indicates the complex source process which radiates strong short period-seismic waves (*e.g.*, Das and Aki, 1977; Campillo, 1983).

SHORT-PERIOD SEISMIC WAVES

Finally we study a short-period seismic wave radiation problem in the frequency domain. Figure 8 shows S-wave acceleration spectra at MYR, OUV and TIS for the 10/4 and 10/9 events. These are obtained for 40 s window of transverse S-wave portion. Spectral shapes are different from site to site, which reflect the different site response. However, the spectral ratios of the 10/4 event to the 10/9 event have common features at these sites as shown in Fig. 9: at low frequencies (f <0.1 Hz) the ratios have a flat level; at frequencies from 0.1 to 2 Hz, the ratios decrease with frequency, except TIS; and at high frequencies (f >2 Hz) the ratios conversely increase.

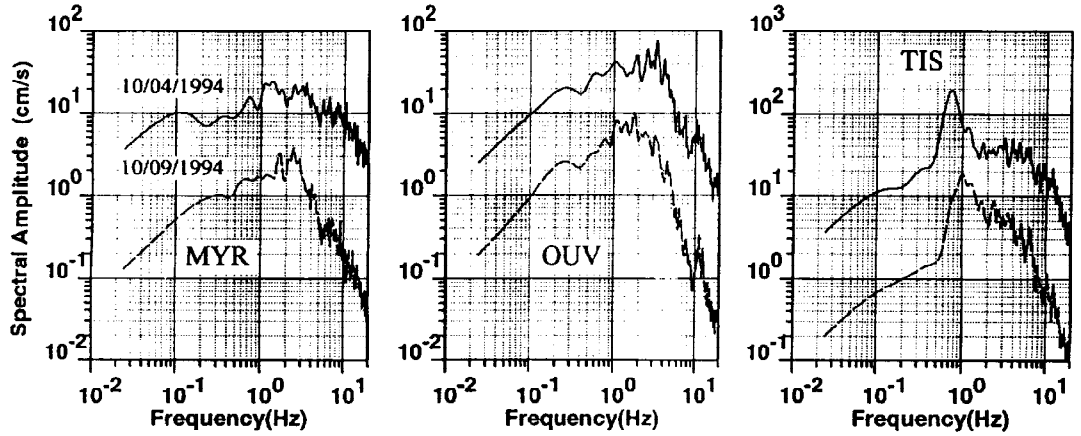

Fig. 8. S-wave acceleration spectra (transverse components) for the 10/4 event (solid curves) and the 10/9 event (dashed curves).

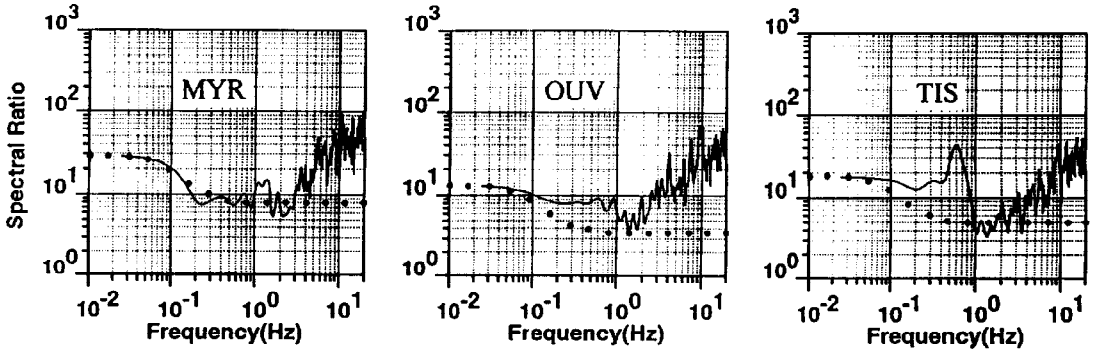

Fig. 9. S-wave spectral ratios (transverse components) of the 10/4 event to the 10/9 event. Dotted curves are reference curves based on the ω^{-2} model.

In order to interpret these features, we shall use reference curves based on the ω^{-2} source model (Singh *et al.*, 1990). For ω^{-2} source model, observed acceleration spectrum can be written as

$$A(f) = C\ G\ Mo\ (2\ \pi\ f)^2\ fo^2\ Q(f)/\ (fo^2 + f^2), \qquad (1)$$

where A(f) = acceleration spectrum, C = source radiation effect, G = geometrical spreading effect, Mo = seismic moment, fo = corner frequency and Q(f) = attenuation effect. The acceleration spectral ratio of event i with respect to event j is given by

$$A_i(f)/A_j(f) = [C_i\ G_i Mo_i\ fo_i^2(f^2 + fo_j^2)]\ /\ [C_j\ G_j\ Mo_j\ fo_j^2\ (f^2 + fo_i^2)] \qquad (2)$$

$$= [C_i\ G_i\ Mo_i]\ /\ [C_j G_j\ Mo_j] \qquad \text{for } f << fo_i,\ fo_j \qquad (3)$$

$$= [C_i\ G_i\ Mo_i]\ /\ [C_j G_j\ Mo_j] \cdot [fo_i^2/fo_j^2]\ . \qquad \text{for } f >> fo_i,\ fo_j \qquad (4)$$

Here we assume $Q_i(f) \sim Q_j(f)$ for the present case. Predicted spectral ratio reference curves for the 10/4 and 10/9 events are shown in Fig. 9. We can use directly the observed, low frequency ratio level for equation (3). In computing fo in equations (2) and (4), we use $fo = \pi/T$(source process time). The reference curves fairly well fit the observed spectral ratios at frequencies from 0.02 to 2 Hz, except TIS: the observed spectral ratio at TIS has a peak at about 6 Hz. At high frequencies (f >2 Hz), all the observed spectral ratios are greater than the reference curve. Although the validity of the ω^{-2} source model for large and great earthquakes at high frequencies is uncertain, this indicates anomalously strong radiation of short-period seismic waves during the 10/4 event. This interpretation may be confirmed by the observed distinct ripples on the vertical velocity seismograms during the 10/4 event as mentioned in the previous section, and explain an extremely large felt area and observed anomalously high peak horizontal accelerations. Aftershock area of the 10/4 event (see Fig. 1) indicates the rupture propagation in the south-west direction. Since our observation sites are located in nearly the same direction, a part of the anomalously strong radiation of short-period seismic waves may be explained by a directivity effect (*e.g.*, Campillo, 1983).

At TIS, the amplitude spectrum for the 10/9 event has a peak at about 1 Hz, but it has a peak at about 7 Hz for the 10/9 event (Fig. 8). The observed spectral ratio peak at about 6 Hz at TIS is apparently due to this peak shift. The peak ground velocity at TIS is 20 cm/s during the 10/4 event, which is about 10 times larger than that (1.7 cm/s) during the 10/9 event. The observed spectral peak shift may be attributed to nonlinear soil response due to strong ground shaking (*e.g.*, Satoh *et al.*, 1992).

CONCLUSIONS

We extracted unique source process of the 1994 Hokkaido Toho-Oki earthquake by comparing wide band strong motion records during main shock and its largest aftershock. The unique points are: 1) large centroid depth, 2) high moment release density, 3) existence of several seconds ripples in the P-wave portion on the vertical velocity records, 4) anomalously strong radiation of short-period seismic waves. Through this analysis, we demonstrate that the wide band strong motion records are very useful to understand the complex source process of large and great earthquakes.

REFERENCES

Campillo, M. (1983). Numerical evaluation of near-field, high-frequency radiation from quasi-dynamic circular faults. *Bull. Seism. Soc. Am.*, **73**, 723-734.

Campillo, M., J. C. Gariel, K. Aki, and F. J. Sanchez-Sesma (1989). Destructive strong ground motion in Mexico city: Source, path, and site effects during great 1985 Michoacan earthquakes. *Bull. Seism. Soc. Am.*, **79**, 1718-1735.

Das, S. and K. Aki (1977). Fault plane with barriers: A versatile earthquake model. *J. Geophys. Res.*, **82**, 5658-5670.

Furumura, M. and T. Sasatani (1996). Secondarily generated surface waves in the Tokachi basin, Hokkaido, Japan. *J. Phys. Earth,* in press.

Iwasaki, T., H. Shiobara, A. Nishizawa, T. Kanazawa, K. Suyehiro, N. Hirata, T. Urabe and H. Shimamura (1989). A detailed subduction structure in the Kurile trench deduced from oceanic seismographic refraction studies. *Tectonophys.*, **165**, 315-336.

Kikuchi, M. and H. Kanamori (1995). The Shikotan earthquake of October 4, 1994: A lithospheric earthquake. submitted to *Geophys. Res. Lett.*

Muramatu, I. (1995). Development of a broadband velocity type strong motion seismometers and its recording range. *Zisin,* **48**, 247-256 (in Japanese).

Sasatani, T. (1966). Site effects in Kushiro during the 1993 Kushiro-Oki and 1994 Hokkaido Toho-Oki earthquakes. *in Special Theme Session on Effect of Surface Geology on Strong Ground Motion, Proc. of 11th World Conference on Earthquake Engineering.*

Satoh, T., T. Sato and H. Kawase (1992). Local site effects on weak and strong ground motions at the Ashigara valley, Japan. *Proc. of International Symposium on Earthquake Disaster Prevention, Mexico,* **Vol. 1**, 227-236.

Singh, S.K., A. Mori, E. Mena, F. Kruger and R. Kind (1990). Evidence for anomalous body-wave radiation between 0.3 and 0.7 Hz from the 1985 September 19 Michoacan, Mexico earthquake. *Geophys. J. Int.*, **101**, 37-48.